Opposite Variability of Indonesian Throughflow and South China Sea Throughflow in the Sulawesi Sea

JUN WEI AND M. T. LI

Laboratory for Climate and Ocean-Atmosphere Studies, and Department of Atmospheric and Oceanic Sciences, Peking University, Beijing, China

P. MALANOTTE-RIZZOLI

Department of Earth, Planetary and Atmospheric Sciences, Massachusetts Institute of Technology, Boston, Massachusetts

A. L. GORDON

Lamont-Doherty Earth Observatory, Columbia University, Palisades, New York

D. X. WANG

South China Sea Institute of Oceanology, Chinese Academy of Sciences, Guangzhou, China

(Manuscript received 2 June 2016, in final form 8 August 2016)

ABSTRACT

Based on a high-resolution (0.1° × 0.1°) regional ocean model covering the entire northern Pacific, this study investigated the seasonal and interannual variability of the Indonesian Throughflow (ITF) and the South China Sea Throughflow (SCSTF) as well as their interactions in the Sulawesi Sea. The model efficiency in simulating the general circulations of the western Pacific boundary currents and the ITF/SCSTF through the major Indonesian seas/straits was first validated against the International Nusantara Stratification and Transport (INSTANT) data, the OFES reanalysis, and results from previous studies. The model simulations of 2004–12 were then analyzed, corresponding to the period of the INSTANT program. The results showed that, derived from the North Equatorial Current (NEC)–Mindanao Current (MC)–Kuroshio variability, the Luzon–Mindoro–Sibutu flow and the Mindanao–Sulawesi flow demonstrate opposite variability before flowing into the Sulawesi Sea. Although the total transport of the Mindanao–Sulawesi flow is much larger than that of the Luzon–Mindoro–Sibutu flow, their variability amplitudes are comparable but out of phase and therefore counteract each other in the Sulawesi Sea. Budget analysis of the two major inflows revealed that the Luzon–Mindoro–Sibutu flow is enhanced southward during winter months and El Niño years, when more Kuroshio water intrudes into the SCS. This flow brings more buoyant SCS water into the western Sulawesi Sea through the Sibutu Strait, building up a west-to-east pressure head anomaly against the Mindanao–Sulawesi inflow and therefore resulting in a reduced outflow into the Makassar Strait. The situation is reversed in the summer months and La Niña years, and this process is shown to be more crucially important to modulate the Makassar ITF's interannual variability than the Luzon–Karimata flow that is primarily driven by seasonal monsoons.

1. Introduction

The Indonesian Throughflow (ITF) is a crucial ocean link, embedded within the Maritime Continent, between the tropical Pacific and Indian Oceans. It originates from tropical Pacific water leaking into the Indonesian seas through the Mindanao–Sulawesi Passage and the Makassar Strait (Gordon et al. 2003) and eventually exported to the Indian Ocean (Gordon et al. 2010). The primary forcing of the export of ITF into the Indian Ocean is derived from the Pacific Ocean pressure head (Sprintall and Revelard 2014; Sprintall et al. 2014). ITF forms an integral part of the interocean exchange, conveying warm and freshwater from the western Pacific Ocean to the eastern Indian Ocean (Gordon 1986, 2001; Sprintall et al. 2013), modifying the thermal and

Lamont-Doherty Earth Observatory contribution number 8043.

Corresponding author address: Dr. Jun Wei, Laboratory for Climate and Ocean-Atmosphere Studies, and Department of Atmospheric and Oceanic Sciences, Peking University, Beijing, China.
E-mail: junwe@pku.edu.cn

DOI: 10.1175/JPO-D-16-0132.1

dynamic structures, as well as the air–sea fluxes within these two tropical oceans.

The South China Sea Throughflow (SCSTF) involves inflow of the Kuroshio into the South China Sea (SCS) through the Luzon Strait and outflow into the Indonesian seas through two major passages: the Karimata Strait and Mindoro–Sibutu Passage. SCSTF represents significant heat and freshwater transport (Qu et al. 2009), receiving heat from the atmosphere with an annual mean of 20–50 W m^{-2} (Yu and Weller 2007) and an annual mean of 0.2–0.3 Sv (1 Sv $\equiv 10^6 m^3 s^{-1}$) rainfall and river runoff (Qu et al. 2009) and transforming cooler and saltier Pacific water into warmer and fresher (more buoyant) outflow into the Indonesian seas. This has been previously recognized to play a potentially important role in modulating the variability of the ITF (Qu et al. 2005; Liu et al. 2006; Tozuka et al. 2009; Qu et al. 2009; Liu et al. 2012; Gordon et al. 2008, 2012; Xu and Malanotte-Rizzoli 2013).

As an early estimate of ITF transport, Godfrey (1989) explicitly derived an ''island rule'' based on a Sverdrup model with simple western boundary layer dynamics, which obtained a transport of 16 ± 4 Sv. Early numerical simulations using global general circulation models (GCMs), although with poor resolutions within the Indonesian seas, yielded mean transports of 12–17 Sv (Semtner and Chervin 1988; Hirst and Godfrey 1993), which was in good agreement with Godfrey's result. Unfortunately, no direct measurements were available at that time to validate these model results. Since the late 1980s, to measure and monitor the mean transport and variability of ITF, several programs have been implemented to observe ITF from its Pacific source, through the Indonesian seas, to the exit passages. Of these programs, the most ambitious international cooperative program is the International Nusantara Stratification and Transport (INSTANT) program (Sprintall et al. 2004).

During the INSTANT program, ITF mean transport and seasonality were measured at the Makassar Strait as 11.6 Sv southward, with a significantly reduced flow in winter and an enhanced flow in summer (Gordon et al. 2008). Early studies suggested that the reduction of ITF can be related to the Wyrtki jet (Wyrtki 1973; Masumoto and Yamagata 1993) and the propagation of Kelvin waves propagation along the coasts of Sumatra and Java (Sprintall et al. 2000; Liu et al. 2011; Pujiana et al. 2013). Another viewpoint in recent studies presumed that the ITF variability can be modulated by the SCSTF outflows. Qu et al. (2005) suggested that the vertical profile in the Makassar Strait is primarily a result of the interplay between the southward-flowing ITF in the thermocline and the northward-flowing SCSTF through the Karimata Strait near the sea surface. The Karimata Strait transport, primarily controlled by the monsoons, shows a flow reversal from winter to summer (Xu and Malanotte-Rizzoli 2013). Based on numerical experiments with and without SCSTF, Tozuka et al. (2007, 2009) found that the observed subsurface velocity maximum of the Makassar ITF was simulated only when SCSTF is allowed in the model to modify the ITF profile through the Karimata Strait flow.

On the interannual time scale, derived from the island rule and Simple Ocean Data Assimilation (SODA) reanalysis, Liu et al. (2006) found that the ITF and SCSTF are always out of phase, controlled by large-scale wind stress. Qu et al. (2005, 2009) and Tozuka et al. (2007, 2009) suggested that the Makassar surface flow is inhibited by the SCSTF outflow through the Karimata Strait during the El Niño years when the Luzon Strait transport is enhanced. On the other hand, Gordon et al. (2012) pointed out that the remote ENSO signals entering the SCS were transferred to the Makassar Strait through the Mindoro–Sibutu Passage, instead of the Karimata Strait, which is mostly driven by seasonal reversed monsoons.

Since both ITF and SCSTF originate from the North Equatorial Current (NEC), separating into the southward-flowing Mindanao Current (MC) and the northward-flowing Kuroshio, their variability is dynamically connected to the NEC–MC–Kuroshio (NMK) system through a series of oceanic passages/straits. The NEC's bifurcation position and variability are subject to both local monsoonal wind forcing and remote forcing of the broad-scale interior ocean via baroclinic Rossby waves (Qiu et al. 2015). NEC bifurcation latitude reaches its northernmost position during winter months and its southernmost position during summer months (Qiu and Lukas 1996; Yaremchuk and Qu 2004; Qiu and Chen 2010). This seasonal migration of the NEC bifurcation was attributed to baroclinic Rossby waves and monsoonal wind forcing near the Philippine coast (Qiu et al. 2015). On the interannual time scales, the NEC's variability can be related to the ENSO events, with a northerly (southerly) bifurcation latitude during the El Niño (La Niña) years (Qiu and Lukas 1996; Qiu and Chen 2010). Accordingly, the Kuroshio and MC transports respond to the changes of the NEC bifurcation latitude, resulting in increasing (decreasing) transports within the Kuroshio and decreased (increased) transports within the MC during La Niña (El Niño) years (Gordon et al. 2014; Kim et al. 2004). For more detailed reviews on the low-latitude Pacific boundary currents, please refer to the special issues of the *Journal of Geophysical Research* (Hu et al. 2015; Schönau and Rudnick 2015) and *Oceanography* (Rudnick et al. 2015; Qiu et al. 2015; Lien et al. 2015).

The Sulawesi Sea is a crucial merging point for the ITF and SCSTF before outflowing into the Makassar Strait and therefore is dynamically important to determine the downstream Makassar ITF variability, which was observed continuously from 2004 to 2012 by the INSTANT program (Gordon et al. 2008, 2012) but has not been fully understood because of the lack of simultaneous measurements of the inflows into the Sulawesi Sea, such as through the Mindoro–Sibutu Passage and from the MC penetration. Existing explanations are derived mostly from model studies. Based on idealized ocean models, the MC penetration into the Sulawesi Sea was interpreted by nonlinear collision of western boundary currents at a gap (Sheremet 2001; Arruda and Nof 2003; Wang and Yuan 2012, 2014). Their results implied that a stronger MC tends to penetrate more deeply into the Sulawesi Sea, with different equilibrium states, depending on the width of the gap. Using a 0.5°, 1.5-layer, reduced-gravity model, Metzger and Hurlburt (1996) examined the circulations connecting the Pacific Ocean, the SCS, and the Sulu Sea, and they found that it is the pressure head created by the pileup of water from the wind stress that controls the Luzon–SCS–Sulu transport. While these studies interpreted respectively on the two inflows into the Sulawesi Sea, Gordon et al. (2012) proposed a "freshwater plug-in" mechanism, elucidating the relationship among the Luzon–SCS–Sulu inflow, the Mindanao–Sulawesi inflow, and the Makassar outflow. They proposed that during La Niña years, less Pacific water enters the Luzon Strait, resulting in more freshwater accumulating in the SCS. During El Niño years, enhanced Luzon–SCS–Sulu inflow forces more fresh SCS water into the Sulawesi Sea through the Mindoro–Sibutu Passage, imposing a west-to-east pressure head against the penetration of the MC and resulting in a reduced outflow into the Makassar Strait.

While this mechanism was partially supported by the INSTANT data (Gordon et al. 2012) and the freshening event of the SCS in a strong La Niña year (Zeng et al. 2014), it has not been examined by any numerical model study. The goal of this study is first to reproduce numerically this mechanism and then to investigate the interaction of the counteracting ITF/SCSTF variability in the Sulawesi Sea. The next section describes the model and data used for this study. Section 3 presents the validation of the model simulations against the reanalysis, observations, and previous studies. Seasonal and interannual variability of the Luzon–SCS–Sibutu flow, the Mindanao–Sulawesi flow, and the Makassar outflow are examined within the Sulawesi Sea based on budget analysis of strait transports. A summary and discussion are given in section 4.

2. Model and data

a. The regional ocean model

The ocean model used in this study is a parallel version of the Princeton Ocean Model (POM), also called Advanced Taiwan Ocean Prediction (ATOP), which was developed specifically by Oey et al. (2013, 2014) for the North Pacific Ocean. The model domain covers 15°S–72°N and 99°E–70°W with a horizontal resolution of $0.1° \times 0.1°$ and includes the entire North Pacific Ocean, the Maritime Continent, and the Indonesian seas/straits (Fig. 1). This domain is semienclosed by three solid boundaries, leaving one major open boundary at 15°S. Along the open boundary, *World Ocean Atlas* (*WOA*) monthly climatological temperature and salinity are specified within a 1.5°-wide relaxation zone (Oey and Chen 1992a,b), and depth-averaged transports are specified from the estimates of Ganachaud and Wunsch (2000), together with a Flather radiation scheme (Oey and Chen 1992a,b).

There are 41 vertical sigma levels with finer resolution near the surface and ocean bottom for better resolving the boundary layers. A fourth-order scheme is adopted to minimize the sigma-level pressure gradient errors (Berntsen and Oey 2010). The topography was interpolated from the ETOPO2 database (http://www.ngdc.noaa.gov/mgg/fliers/01mgg04.html). The Mellor and Yamada level-2.5 turbulent closure scheme is used for vertical eddy viscosity and diffusivity (Mellor and Yamada 1982) and the Smagorinsky turbulence closure is used for horizontal diffusivity (Smagorinsky 1963). The model was spun up since 1986, driven by the 6-hourly NCEP surface flux (wind, heat, and mass), and a bulk wind stress formula was used for the drag coefficient (Oey et al. 2006, 2007). The model simulations during 2004–12 (corresponding to the INSTANT period), which is already in a statistical equilibrium in terms of its total kinetic energy, were used for analysis in this study. Further details of the model configurations and validations, especially in the South China Sea and the open oceans, are provided in Oey et al. (2013, 2014).

b. Data

In this study, the model results were first validated against the INSTANT measurements, OGCM for the Earth Simulator (OFES) reanalysis, and results from previous studies. The INSTANT program was initialized in August 2003 and reached the full mooring array in January 2004. This program measured ITF's velocity, salinity, and temperature simultaneously in the Makassar Strait, Lifamatola Passage, Lombok Strait, Ombai Strait, and Timor Passage (Sprintall et al. 2004; Gordon et al. 2010). Specifically, the Makassar Strait Throughflow was intensively measured by two moorings at 2.86°S and 118.46°E/118.62°E within the 45-km-wide Labani Channel from January 2004 to late November 2006 (Gordon et al. 2008), and the western mooring was maintained during the follow-up MITF program until July 2011 (Gordon et al. 2012). These multiyear, simultaneous moorings within the Indonesian seas/straits provide

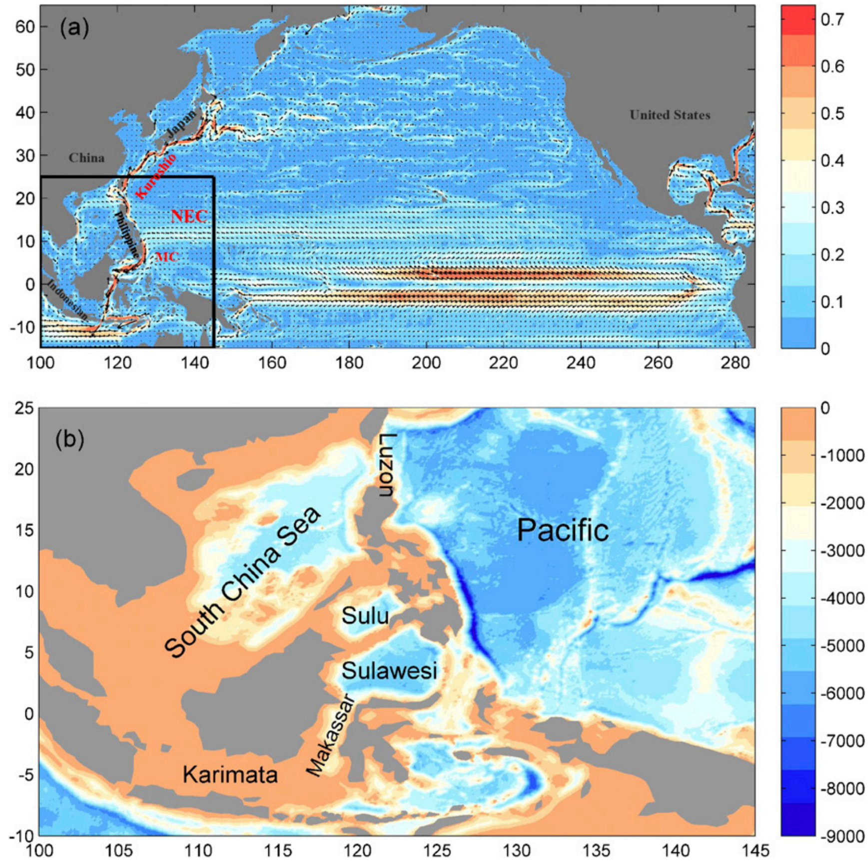

FIG. 1. (a) ATOP model domain (black box) and 8-yr-averaged (2004–12) surface velocity field ($m\,s^{-1}$) and (b) the major internal seas and straits in the Maritime Continent.

valuable data to study the ITF transport and its variability on seasonal to interannual time scales.

Since there is lacking of simultaneous measurements in the upstream straits, such as the Mindoro Strait, the Sibutu Strait, and the eastern entrance of the Sulawesi Sea, we used the OFES reanalysis as a reference, which has the same resolution of 0.1°. OFES is a high-resolution, eddy-resolving, global OGCM (excluding arctic regions), developed by the Japan Agency for Marine-Earth Science and Technology (JAMSTEC). It provides decadal simulations from 1950 to the present year, which has been commonly used for the studies in the western Pacific Ocean (Masumoto et al. 2004). The SODA (version 2.2.4; Carton et al. 2000) reanalysis (http://www.atmos.umd.edu/~ocean/) is also used to verify the simulated ITF vertical velocity profile at the Makassar Strait. The SODA reanalysis is a data assimilation product with a resolution of 0.5° × 0.5° in longitude and latitude in the tropics, combining all the worldwide available observations at all ocean depths with the GFDL Parallel Ocean Program (POP) global ocean circulation model for the period of 1890–2010.

3. Results

a. Validation of the ATOP model

The model validation in the Indonesian seas/straits is always challenging because of very limited and sparse measurements in both space and time scales. Following most of the previous numerical studies, which often used global OGCM reanalysis datasets or earlier model results as a reference (Metzger and Hurlburt 1996; Qu et al. 2004; Kim et al. 2004; Tozuka et al. 2009; Liu et al. 2011; Xu and Malanotte-Rizzoli 2013), in this section we first validate the ATOP model with the INSTANT data, the results from earlier studies, and the OFES reanalysis. To be consistent with the INSTANT data, the model simulations during 2004–12 were analyzed. Figure 2 compares the ATOP 8-yr-averaged sea surface height anomaly (SSHA) and depth-averaged velocity to the OFES reanalysis. Both models show an evident NEC that separates at the Philippine coast between 12° and 13°N, with its northward branch (Kuroshio) intruding into SCS forming the SCSTF and its southward branch (MC) leaking into the Makassar Strait forming

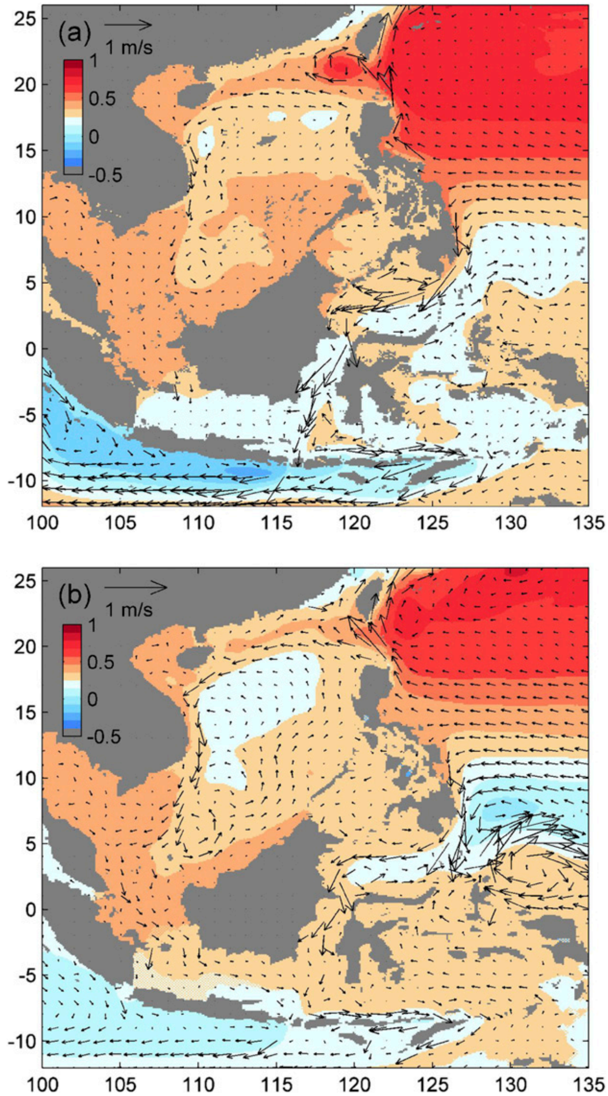

FIG. 2. Comparison of time-averaged (2004–12) SSHA and depth-averaged velocity fields between (a) the ATOP model and (b) the OFES model.

the ITF. In particular, the ATOP model produces a stronger ITF at the Makassar Strait than that in the OFES. The ITF transport estimated from the ATOP model is ~12 Sv, comparable to the INSTANT data (11.6 Sv), while the ITF in OFES is underestimated by about 50% (~6.6 Sv). This is likely because the OFES model resolves a strong anticyclonic New Guinea Coastal Current (NGCC), colliding with the MC at the eastern Sulawesi, inhibiting the MC penetration into the Sulawesi Sea, and thus leading to a weak ITF (Arruda and Nof 2003; Wang and Yuan 2014). In contrast, the NGCC in the ATOP model is relatively weaker and more MC water leaks into the Sulawesi Sea.

The model efficiency in simulating the ITF and SCSTF can be assessed by comparing strait transports

TABLE 1. Comparison of ATOP transport with previous studies/observations. Note that the positive/negative signs indicate northward/eastward and southward/westward flow, respectively.

Straits	Transport (Sv)	References/periods
North Equatorial Current	−47	This study/2004–12
	−41	Qu et al. (1998)/1986–90
	−55	Qiu and Lukas (1996)/1961–92
	−38	OFES/2004–12
Kuroshio	28	This study/2004–12
	14	Qu et al. (1998)/1986–90
	30	Qiu and Lukas (1996)/1961–92
	17	OFES/2004–12
Mindanao Current	−17	This study/2004–12
	−27	Qu et al. (1998)/1986–90
	−25	Qiu and Lukas (1996)/1961–92
	−20	OFES/2004–12
Luzon Strait	−4.9	This study/2004–12
	−6.0	Tian et al. (2006)/October 2005
	−5.2	Hurlburt et al. (2011)/2004–09
	−4.5	Xu and Malanotte-Rizzoli (2013)/1960s
	−4.0	OFES/2004–12
Karimata Strait	−0.7	This study/2004–12
	−1 to −2	Wyrtki (1961)
	−0.58	Gordon et al. (2012)/2004–11
	−1.4	Xu and Malanotte-Rizzoli (2013)/1960s
	−1.0	OFES/2004–12
Mindoro Strait	−2.6	This study/2004–12
	−2.4	Qu and Song (2009)/2004–07
	−2.0	Xu and Malanotte-Rizzoli (2013)/1960s
	−3.1	Metzger and Hurlburt (1996)/1982–83
	−1.6	OFES/2004–12
Sibutu Strait	−2.9	This study/2004–2012
	−1.62	Gordon et al. (2012)/2004–11.09
	−2.8	Qu and Song (2009)/2004–07
	−2.9	Xu and Malanotte-Rizzoli (2013)/1960s
	−1.6	OFES/2004–12
Mindanao–Sulawesi	−16	This study/2004–12
	−16 ± 4	Godfrey (1989)
	−14.3	OFES/2004–12
Makassar Strait	−12	This study/2004–12
	−9.6	Xu and Malanotte-Rizzoli (2013)/1960s
	−9.9	Metzger and Hurlburt (1996)/1982–83
	−11.6	Gordon et al. (2008)/2004–06
	−6.6	OFES/2004–12

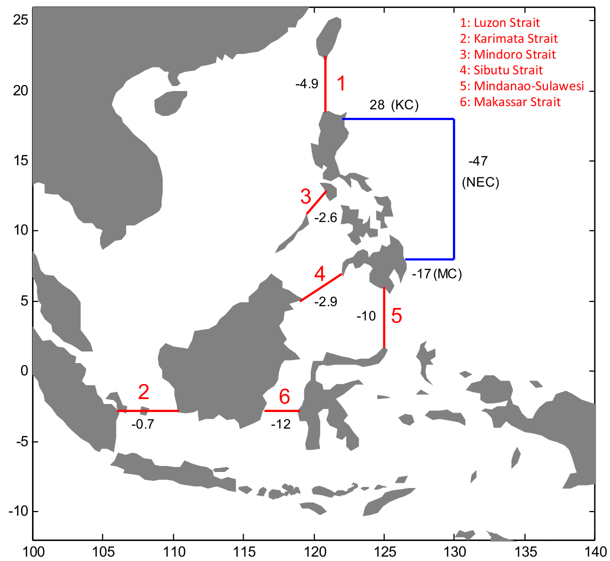

FIG. 3. Time-averaged (2004–12) transports calculated from ATOP results at the major straits (marked as black numbers; Sv). Note that positive values indicate northward/eastward flows and negative values indicate southward/westward flows. Straits 1–6 (red) denote the crucial SCSTF and ITF pathways, which were specifically examined in this study.

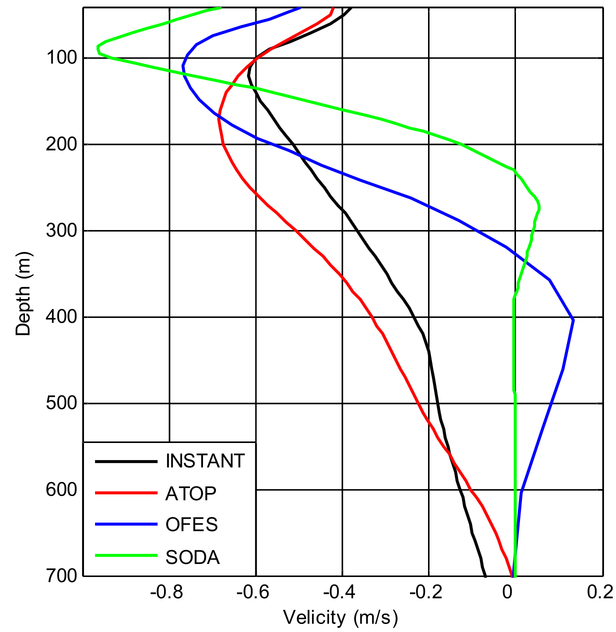

FIG. 4. Time-averaged (2004–12) vertical velocity profiles at the Makassar Strait calculated from INSTANT–MITF measurements, the ATOP model, the OFES model, and SODA reanalysis.

along their pathways. Table 1 summarizes the strait transports and their periods from the INSTANT data, the OFES reanalysis and the previous studies. Note that positive and negative signs in transports indicate northward/eastward and southward/westward flows, respectively. As shown, ATOP produces correct directions of the throughflows at all straits, with reasonable transports compared to the references. It is noteworthy that although the resolutions of all models in the Table 1 are not fine enough to resolve accurately the Mindoro–Sibutu Straits, their simulated mean transports are consistent. Figure 3 presents the ATOP mean transports for the NMK currents and at the straits connecting to the Sulawesi Sea. The Mindanao–Sulawesi flow (10 Sv) appears to contribute largely to the total ITF transport (12 Sv). The Luzon Strait transport is 4.9 Sv into the SCS and outflows the SCS Basin from the Taiwan Strait (1.1 Sv, not shown), the Karimata Strait (0.7 Sv), and the Mindoro–Sibutu Strait (2.6–2.9 Sv). In terms of these mean transports, the ATOP model is able to produce a reasonable estimate, compared to the previous results.

The model also reproduces reasonably the vertical profile at the Makassar Strait, which carries 80% of the total ITF transport estimated from the INSTANT data (Gordon et al. 2010). Figure 4 compares the vertical velocity profiles from the INSTANT measurements, the ATOP model, and OFES and SODA reanalysis averaged over 2004–12. The observed profile demonstrates a southward flow with a subsurface velocity maximum of $0.64\ \mathrm{m\,s^{-1}}$ at about 120-depth. The flow velocity decreases to $0.4\ \mathrm{m\,s^{-1}}$ at surface and vanishes at approximately 700-m depth. The ATOP model can generally reproduce the observed profile, with a relatively deeper velocity core. It shows that both SODA and OFES reanalysis not only overestimate the subsurface velocity maximum, but also fail to resolve the deep flows below 300 m, which results in an underestimated ITF transport at the Makassar Strait (Fig. 2b). Note that SODA is another global reanalysis data, with a coarser resolution of 0.25° (Carton et al. 2000).

b. *Seasonal variability of ITF and SCSTF in the Sulawesi Sea*

The transport of the ITF and SCSTF entering the Sulawesi Sea depends on the variability of the Luzon–Mindoro–Sibutu/Mindanao–Sulawesi inflows, as stronger Kuroshio and MC tend to penetrate more deeply into the western basins (Sheremet 2001; Wang and Yuan 2014). On the other hand, partitioning of the Kuroshio/MC transport from the NEC is associated partially with the seasonal migration of the NEC bifurcation latitude (Qiu and Lukas 1996; Kim et al. 2004). Figure 5 shows 8-yr-averaged horizontal flow fields in winter [December–February (DJF)] and summer [June–August (JJA)]. It appears that there is greater intrusion of Kuroshio water into the Luzon Strait and less MC into the Sulawesi Sea in the winter season, corresponding to a more northern position of the NEC bifurcation latitude. As a result, the SCSTF is enhanced, turning anticlockwise around

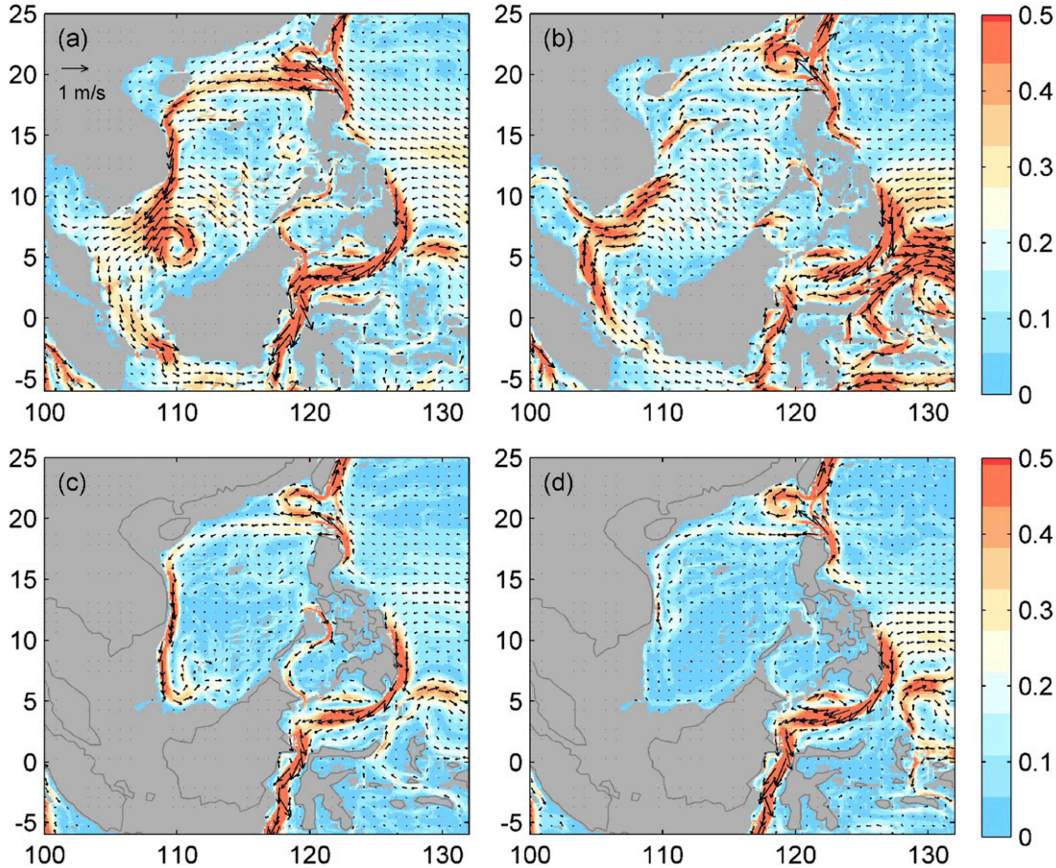

FIG. 5. Time-averaged (2004–12) velocity fields in winter (JFM) (a) at the surface and (c) at 150-m depth and in summer (JAS) (b) at the surface and (d) at 150-m depth. Color shadings indicate current speeds [m s^{-1}, $(u^2 + v^2)^{1/2}$].

the SCS Basin and then outflowing into the Karimata Strait at the surface only (Fig. 5a) and through the Mindoro–Sibutu Passages down to 150-m depth (Fig. 5c). Note that, in contrast to the southward Mindoro–Sibutu flow, the Karimata Strait flow changes its direction with seasonal reversing monsoons, with a northward flow (into the SCS) in winter (Fig. 5a) and a southward flow (into the Java Sea) in summer (Fig. 5b). Despite a lack of long-term measurements at the Mindoro–Sibutu Passage, this southward flow has been estimated by previous studies, ranging from 1.6–3.1 Sv (Table 1), which is larger than the Karimata flow, implying its potentially important role in modulating the Makassar ITF variability—not only through the Karimata Strait, as previously thought (Qu et al. 2005; Tozuka et al. 2007, 2009), but also through the Mindoro–Sibutu Passage, as first proposed by Gordon et al. (2012).

Figure 6 shows seasonal cycles of the NMK and the SCSTF/ITF transports at the key straits. To highlight their seasonality, mean flows were removed from all transports, so that the variability amplitudes can be compared directly. By doing so, positive values indicate northward/eastward flow anomalies, and negative values indicate southward/westward flow anomalies. For the NMK currents, the NEC shows evident seasonality in terms of its mean transport and bifurcation latitude. It moves to its northernmost position in January, corresponding to its minimal transport, and reaches its southernmost position in June, with maximum transport in August. Accordingly, the Kuroshio shows a similar seasonal cycle to the NEC, but with a reduced amplitude of variability (Fig. 6b), while the MC shows an opposite cycle, with a maximum/minimum southward transport in April/September (Fig. 6c), reflecting a transport compensation between these two boundary currents. This is well consistent with the general variability of the NMK, shown in previous studies (Qiu and Lukas 1996; Kim et al. 2004). For the SCSTF, the transports at the Luzon, Karimata, Mindoro, and Sibutu Straits all show a seasonality with a maximum/minimum transport in the winter/summer months and amplitudes of 3–4 Sv. In contrast, the ITF seasonality through the Mindanao–Sulawesi Passage shows an amplitude of 5.6 Sv. This implies that although

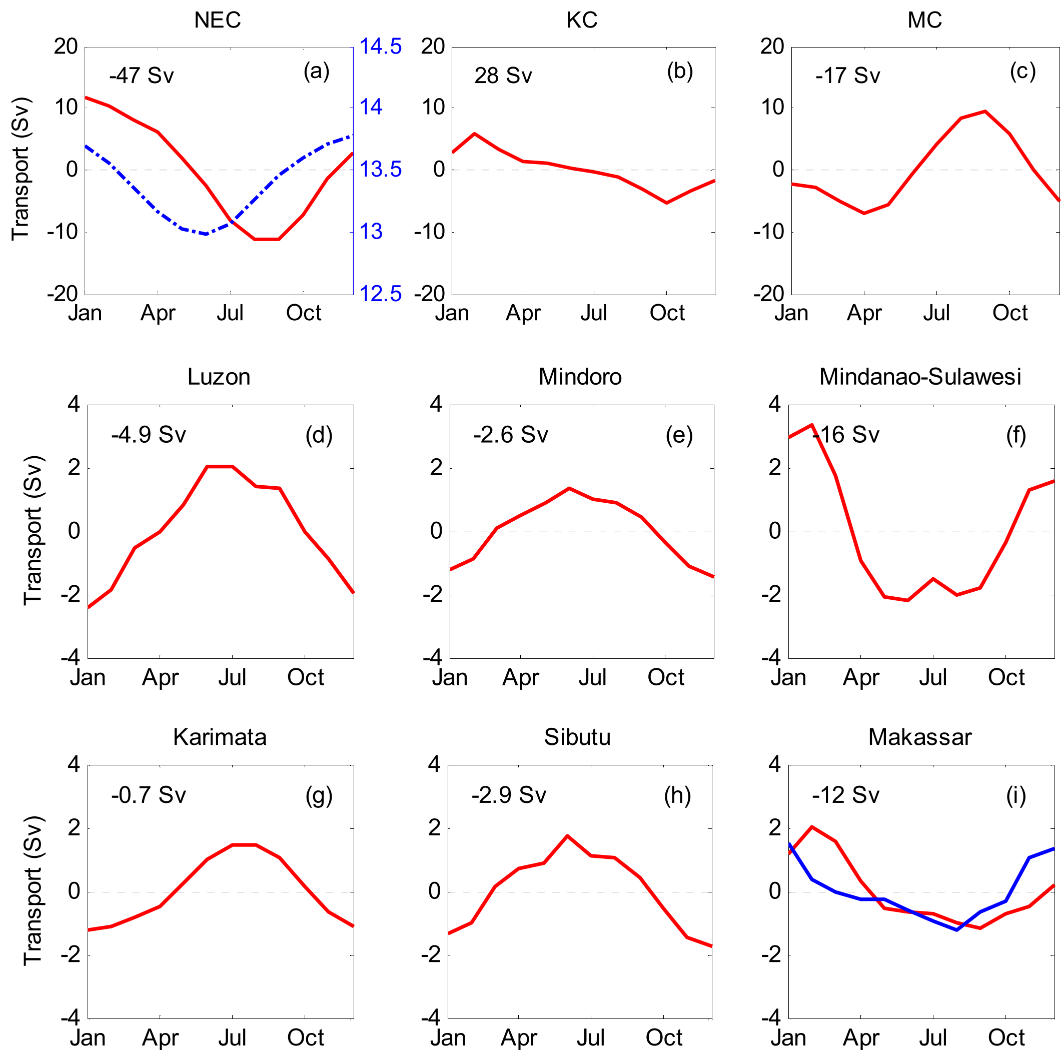

FIG. 6. Seasonality of NEC–MC–Kuroshio and SCSTF/ITF at the major straits (see Fig. 3 for locations). Mean flows were marked in each subplot but removed from all transports; thus, positive values indicate northward/eastward flow anomalies and negative values indicate southward/westward flow anomalies. For comparison, the seasonality of NEC bifurcation positions (blue) and the observed INSTANT–MITF transport (red) are superimposed on (a) and (i), respectively.

the SCSTF mean flow is much smaller than that of the ITF, their seasonality amplitudes are actually comparable. Most importantly, derived from the opposite Kuroshio/MC currents, the seasonality of the SCSTF and ITF are out of phase too, which counteract with each other in the Sulawesi Sea and result in a subdued seasonality of 2.8 Sv at the Makassar Strait. This resultant Makassar ITF seasonality reasonably reproduces the observed seasonal cycle estimated from the INSTANT measurements (blue line in Fig. 6i).

To examine the interaction/counteraction of the SCSTF and ITF inflows in the Sulawesi Sea, Fig. 7a displays the model time-averaged (2004–12) SSHA. The SSHA isolines clearly mark the ITF pathway that originates from the MC leaking into the Sulawesi Sea (solid purple line) and the cyclonic SCSTF pathway surrounding the SCS Basin, outflowing through the Mindoro–Sibutu Passage (dash blue line). Both pathways generally follow the SSHA isoline of 0.3 m, indicating their geostrophy in most areas in the Indonesian seas (Burnett et al. 2003). The two throughflows, which carry opposite seasonality, enter the Sulawesi Sea and thus counteract with each other before outflowing to the Makassar Strait. It is shown that cross-isoline gradients are weakened greatly in the Makassar Strait located near the equator, indicating that the Makassar ITF is not controlled by the geostrophic balance, but the resultant of pressure forces between the Pacific Ocean

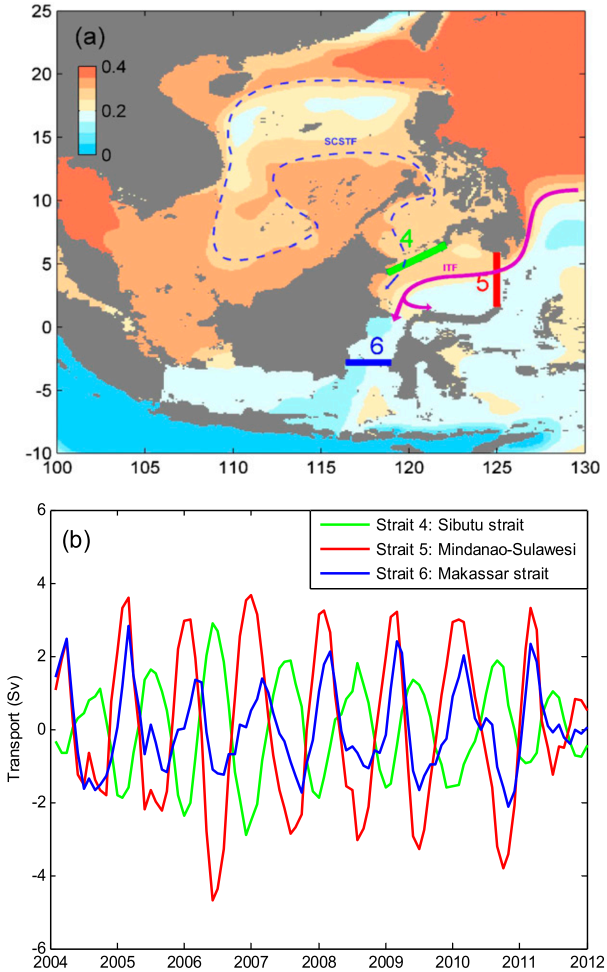

FIG. 7. Box budget analysis for seasonality of the throughflows in the Sulawesi Sea: (a) time-averaged (2004–12) SSHA (m) and (b) seasonal evolutions of transport at the Sibutu, Mindanao–Sulawesi, and Makassar Straits. Note that 12-month running means were removed from the transports to highlight their seasonality.

and the Indian Ocean, the so-called pressure head (Burnett et al. 2003; Kamenkovich et al. 2003, 2009). On the other hand, the SSHA gradient along the Karimata Strait is weak too, indicating that the Karimata flow is not controlled by the geostrophic balance too but the local reversing monsoons (Qu et al. 2005). Figure 7b presents seasonal evolutions of the three in-/outflows of the Sulawesi Sea from 2004 to 2012. The opposite seasonality of the Mindanao–Sulawesi flow and the Mindoro–Sibutu flow is remarkable, with a correlation coefficient of −0.9, which results in a subdued seasonality for the Makassar outflow (blue line). This negative correlation coefficient is largest (−0.924) at 1-month lag (Sibutu flow leads the Mindanao–Sulawesi flow), implying the modulations of the Mindoro–Sibutu Throughflow on the Mindanao–Sulawesi inflow.

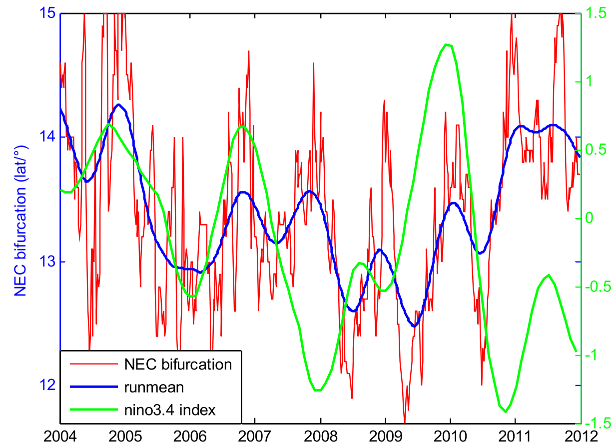

FIG. 8. Comparison of model NEC bifurcation and the Niño-3.4 index. The red line is the model 5-day result, and the blue line is the 6-month running mean.

c. *Interannual variability of SCSTF and ITF in the Sulawesi Sea*

The interannual variability of the SCSTF and ITF has been previously related to remote ENSO signals transferred into the SCS and Indonesian seas through the NMK boundary currents (Qiu and Lukas 1996; Liu et al. 2006; Gordon et al. 2012; Qiu et al. 2015). Figure 8 compares the model NEC bifurcation and the Niño-3.4 SST index during 2004–12. A 6-month running mean was applied to the 5-day model outputs to filter out subseasonal signals. First, the south–north seasonal migration of the NEC bifurcation is prominent, except for the 2005/06 winter when the NEC moved south, instead of north as it did in all other winters. This is most likely modulated by the 2005/06 La Niña event, in which the NEC tended to stay in a more southern position (Qiu and Lukas 1996). Second, the NEC bifurcation also shows prominent interannual variations, following generally the Niño-3.4 index, with the exception of the 2007/08 winter when the NEC tended to stay in a more northern position. For the rest of the years, the model is able to simulate the south–north migration of the NEC bifurcation that is a combination of its seasonality and the ENSO signals.

One can readily expect that the interannual ENSO signals can be transferred into the Sulawesi Sea through the Luzon–Mindoro–Sibutu and the Mindanao–Sulawesi flows. Figure 9 shows the correlation coefficients between individual strait transport and the Niño-3.4 index. The Luzon–Mindoro–Sibutu transport is negatively correlated with the ENSO index, with a correlation coefficient from −0.67 to −0.79, while the correlation coefficient of the Mindanao–Sulawesi flow is positive (0.61). This result is consistent with Gordon

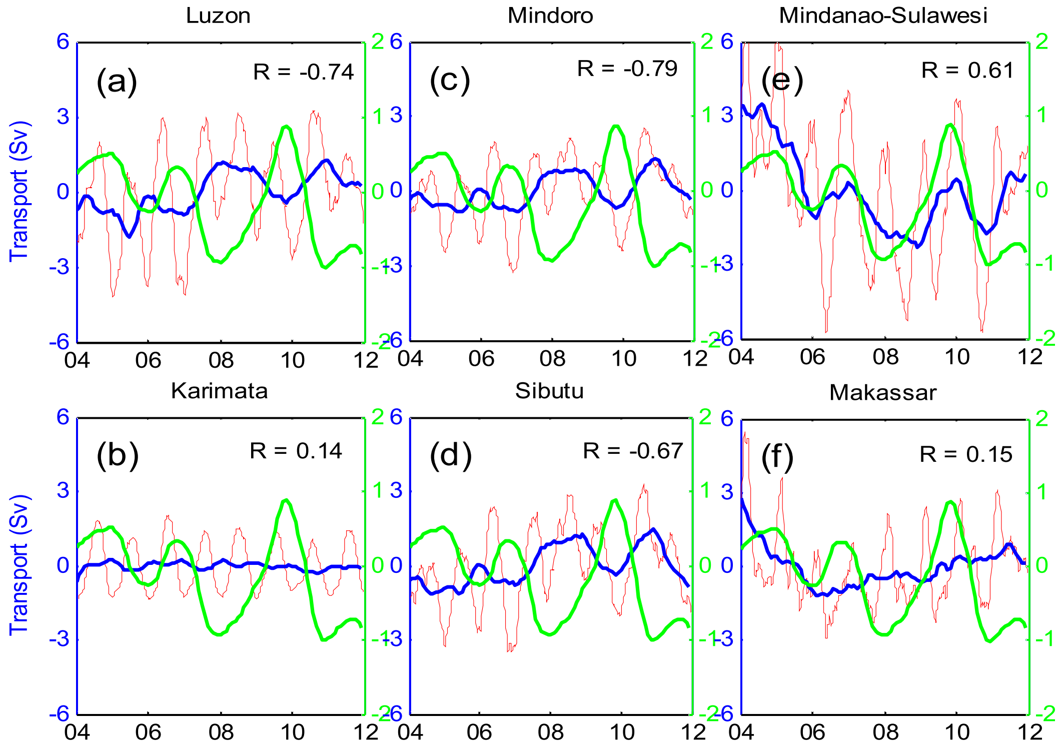

FIG. 9. Interannual variability of the transports at the major strait. The Niño-3.4 index is plotted for reference (green lines). The red lines are monthly averaged results, and blue lines are the 12-month running means, used to filter out seasonal variations. Correlation coefficients between blue lines and green lines are marked.

et al. (2012), based on global HYCOM reanalysis. However, the ENSO signal becomes insignificant at the Karimata Strait, where the flow variability is controlled by the reversing monsoons, with no significant interannual variations (Fig. 9b). This implies that the interannual variability of the Makassar ITF is determined by a combination of the Mindanao–Sulawesi and Mindoro–Sibutu inflows, while the modulation from the Karimata flow is negligible.

To demonstrate the interannual interaction of the Mindanao–Sulawesi and Mindoro–Sibutu inflows in the Sulawesi Sea, Fig. 10 presents composite SSHA for all La Niña years (2005/06, 2007/08, 2008/09, and 2011/12) and the SSHA difference between all El Niño years (2004/05, 2006/07, and 2009/10) and all La Niña years. In La Niña years (Fig. 10a), the NEC bifurcates at a more southern latitude than in the El Niño years (Qiu and Lukas 1996). As a result, less Kuroshio water intrudes into the SCS, leading to a weaker Mindoro–Sibutu flow. In Fig. 10b, the SSHA difference indicates an enhanced southward Mindoro–Sibutu flow in El Niño years. On the other hand, along the eastern coast of the Philippine Island, the SSHA isolines indicate an evident southward-flowing flow anomaly, which decreases the northward-flowing Kuroshio and increases the southward-flowing MC. This flow anomaly indicates that, with respect to the NEC bifurcation latitude in La Niña years, the NEC moves to a more northern latitude during El Niño years. Furthermore, within the Sulawesi Sea, the SSHA difference (El Niño years − La Niña years) shows a west-to-east pressure head anomaly, which pushes the MC retroflection back to the Pacific (Fig. 10b).

Note that the geostrophic component of the ITF in the Sulawesi Sea is maintained primarily by north-to-south pressure gradients balanced by the Coriolis force, while Fig. 10b implies that the enhanced Mindoro–Sibutu inflow during the El Niño years builds up a west-to-east pressure anomaly against the MC penetration. To examine the variability of the west-to-east pressure anomaly, Fig. 11a shows the SSH difference between the western and eastern Sulawesi Sea separated by 122°E. It appears that this SSH anomaly is highly correlated with the Niño-3.4 index, with a correlation coefficient of 0.77. Its dynamical interpretation has been given by Gordon et al. (2012) related to the ENSO events; during the La Niña years, the freshwater is accumulating in the SCS with reduced Kuroshio intrusion into the SCS. During the El Niño years, enhanced Luzon Strait flow brings more SCS water into the western Sulawesi Sea through

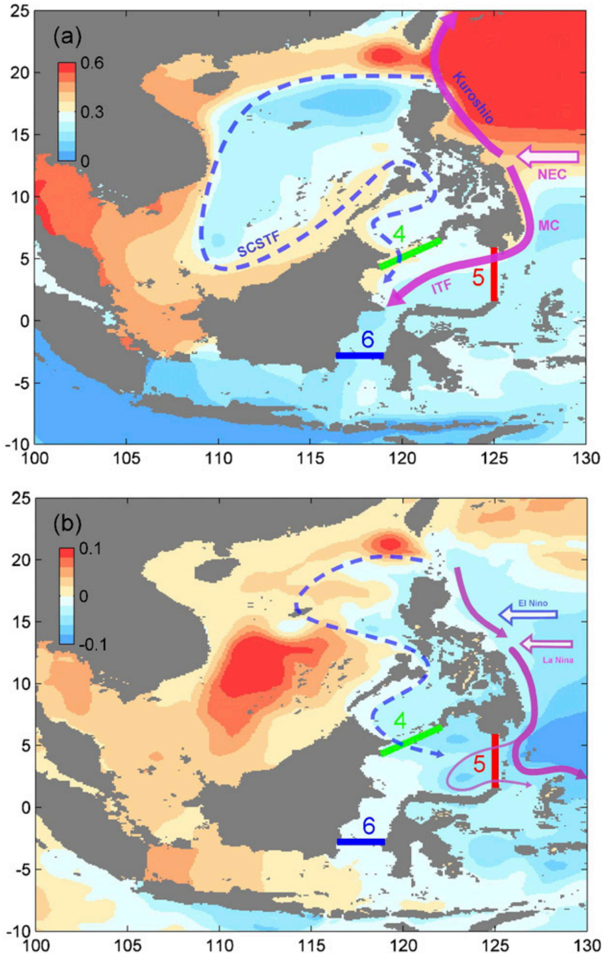

FIG. 10. (a) Composite SSHA (m) for all La Niña years (2005/06, 2007/08, 2008/09, and 2011/12) and (b) composite SSHA difference (m) between all El Niño years (2004/05, 2006/07, and 2009/10) and all La Niña years (El Niño − La Niña).

the Sibutu Strait, building a positive west-to-east pressure head. Figures 11b and 11c show composite annual variations of the Sibutu flow, Mindanao–Sulawesi flow, and Makassar flow for all La Niña and El Niño years, respectively. Given that the ENSO events reached their maximum strength during winter months (Fig. 8), the strait transport cycles are centered in January. The three flows are dominated by their seasonality, as described in Fig. 7b. Meanwhile, we see that the southward Sibutu flow (green line) is increased on average by 1.2 Sv in the El Niño years (Fig. 11b), comparing to the La Niña years (Fig. 11c), while the westward Mindanao–Sulawesi flow (red lines) is reduced by 2.4 Sv. This is consistent with the schematics of the interaction of the two inflows, shown in Fig. 10b. To compensate the changes of these two inflows into the Sulawesi Sea, the Makassar outflow is reduced accordingly.

4. Summary and discussions

Based on a high-resolution (0.1° × 0.1°) regional ocean model covering the entire northern Pacific, this study investigated the interaction of seasonal and interannual variability of the SCSTF and ITF in the Sulawesi Sea. The model efficiency in simulating the general variability of the NMK currents and the ITF/SCSTF along the major straits/seas was first validated against the INSTANT data, OFES reanalysis, and results from previous studies. The model simulations of 2004–12 were then analyzed, corresponding to the mooring period of the INSTANT program. The results showed that, derived from the NMK circulations, the Luzon–Mindoro–Sibutu flow and the Mindanao–Sulawesi flow demonstrate opposite variability before they enter the Sulawesi Sea. Although the Mindanao–Sulawesi flow mean transport is much larger than that of the Luzon–Mindoro–Sibutu flow, their variability amplitudes are comparable but out of phase, and therefore the two inflows counteract with each other within the Sulawesi Sea before entering the Makassar Strait. Budget analysis of the volume transports of these in-/outflows revealed that the southward Luzon–Mindoro–Sibutu flow is enhanced during winter months and El Niño years. As a result, more buoyant SCS water accumulates in the western Sulawesi Sea, building up a west-to-east pressure head against the Mindanao–Sulawesi flow into the Sulawesi Sea. The situation is reversed in the summer months and La Niña years, and this process is shown to be crucially important to determine the seasonal and interannual variability of the downstream Makassar ITF.

The interaction of the ITF and SCSTF is embedded in the Indonesian seas, which consist of multiple narrow straits/passages and internal seas of varying dimensions. This remains one of the major challenges to simulate accurately the throughflow structures and their variability. Not only high resolution but also many other factors (i.e., model configurations and parameterizations) need to be appropriately addressed. Van Sebille et al. (2014) adopted a 0.1° regional model (NEMO), emphasizing the southern Maritime Continent and obtaining a good estimate of ITF transport and its variability. A more recent study by Tranchant et al. (2016) included tides in a regional high-resolution model for the Indonesian seas [INDO12 (1/12° resolution)], and the model is capable of simulating accurately complex elevations (amplitudes and phase) and water properties within the Indonesian Straits, which agreed well with in situ observations. Given that the new objective of this study is on the seasonal and interannual variability, we did not include tides in ATOP. Instead, we adopted a

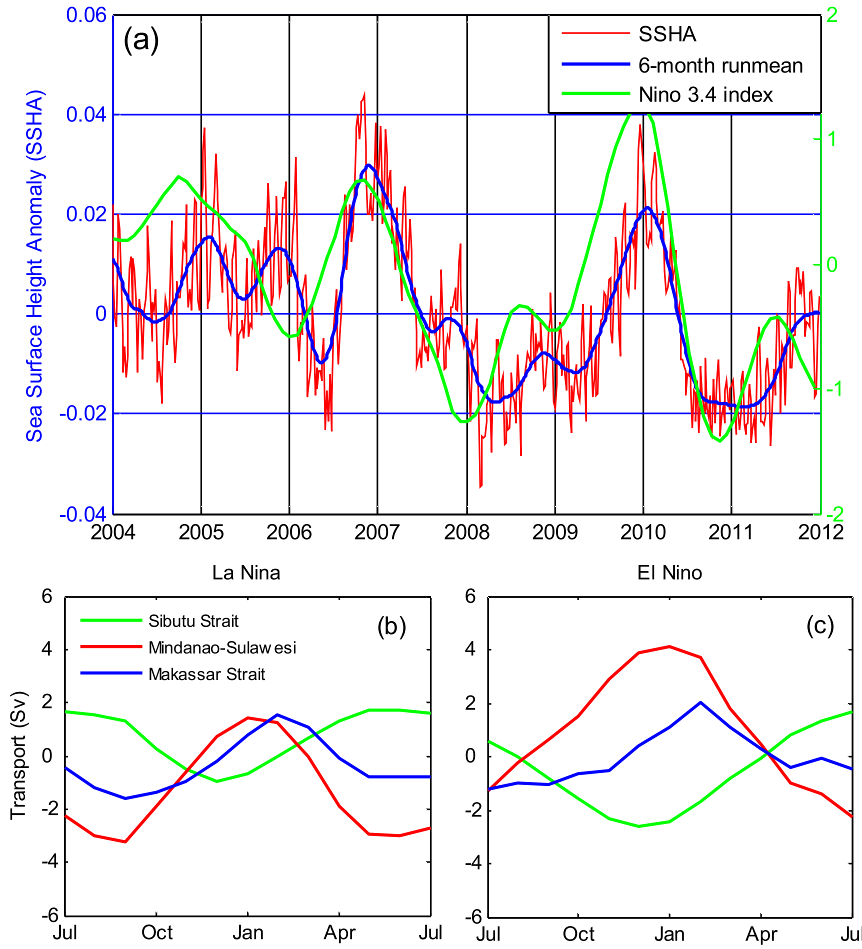

FIG. 11. Box budget analysis of the throughflows in the Sulawesi Sea: (a) west-to-east SSH gradient in the Sulawesi Sea separated by 122°E, (b) composite flow cycles for all La Niña years (2005/06, 2007/08, 2008/09, and 2010/11) and (c) composite flow cycles for all El Niño years (2004/05, 2006/07, and 2009/10).

large Pacific model and a 0.1° resolution over the entire domain, so that we were able to simulate simultaneously the seasonal and interannual variability driven by the local processes and the remote forcing transferred from the Pacific interior to the Maritime Continent. Although ATOP does not include tides, it produces the total transports comparable with those of the other high-resolution models. Note that the OFES reanalysis, which has the same resolution of 0.1°, is shown to be unable to simulate correctly the vertical profile (Fig. 4) and the ITF transport compared to the above recently developed models and the INSTANT data (Fig. 12).

Although direct measurements within the NMK and the SCSTF/ITF currents are lacking, Zhang et al. (2014) and Hu et al. (2016) recently presented 4-yr moored ADCP data for the MC at 8°N, 127°E. In their studies, observed, depth-dependent velocities suggested that strong and lower-frequency variability dominates the upper-layer MC, and weak and higher-frequency fluctuation controls the subsurface MUC, which was attributed to multiple driving forcing, for example, westward-propagating Rossby waves, wind forcing, and local Ekman pumping. Although the two studies emphasized respectively on the intraseasonal and interannual time scales, Zhang et al. (2014) found that the upper MC (down to 600-m depth) is weakest in the fall months and peaks in the spring months (their Fig. 11a), which is generally consistent with our model results (Fig. 6c). For the interannual time scale, our results suggest that the correlation coefficient between the MC variability and Niño-3.4 index is 0.61, but no significant relation is found in the ADCP data (Hu et al. 2016), which is likely because the ENSO signal is weak during the mooring measurement period.

The Makassar Strait has been previously thought to be the merging point for the SCSTF and ITF, where the

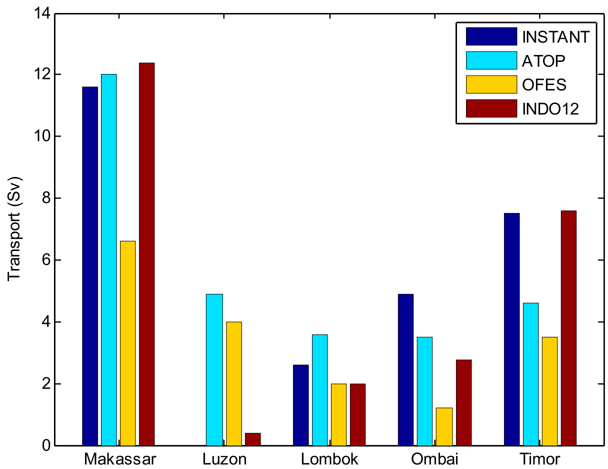

FIG. 12. Comparison of simulated throughflow transports in the key straits between ATOP, OFES, and INDO12 models. The observed transports from the INSTANT project are marked for references.

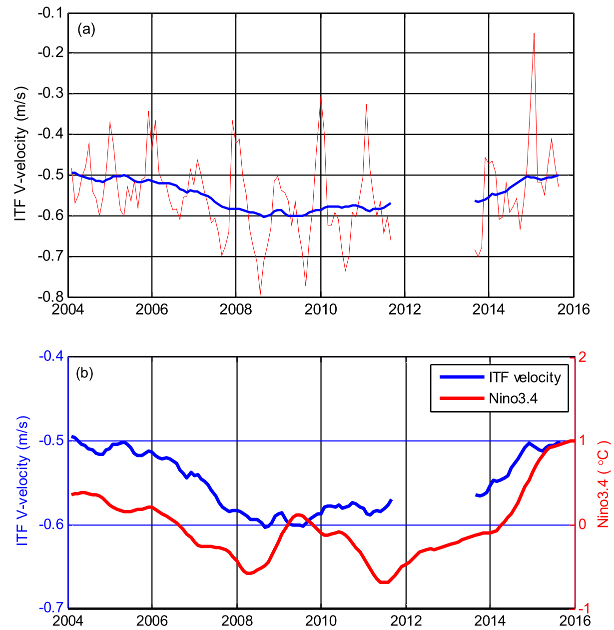

FIG. 13. (a) ITF seasonality of v-component velocity and its 12-month running mean from the INSTANT project and (b) 12-month running means of the ITF v velocity and Niño-3.4 index. Note that the INSTANT data are missing during September 2011 to July 2013 due to no mooring deployed.

SCSTF through the Karimata Strait reduces/increases the total ITF in winter/summer (Qu et al. 2005; Tozuka et al. 2007, 2009). While the monsoon-driven Karimata flow contributes to the Makassar ITF seasonality, it plays an insignificant role in modulating the ITF interannual variability. In this study, it is revealed that both seasonal and interannual ITF variability are modulated by the SCSTF through the Mindoro–Sibutu Passage before entering the Makassar Strait. The Mindoro–Sibutu flow carries an opposite variability with the Mindanao–Sulawesi flow, and the two flows merge together in the Sulawesi Sea. For seasonal variability, the Mindoro–Sibutu flow is derived from the Luzon Strait transport, with an opposite seasonality with the Mindanao–Sulawesi flow, derived from the MC variability. This results in a subdued seasonality of the downstream Makassar ITF. For the interannual variability, the Mindanao–Sulawesi flow is largely influenced by the ‘‘ENSO-like’’ west-to-east pressure head, created by the Mindoro–Sibutu flow with a variability amplitude of 2.9 Sv, instead of from the long pathway of the Karimata Strait (0.7 Sv).

The ‘‘pressure head’’ was explicitly defined as the difference of total pressure forces acting on the Indonesian seas waters from the western Pacific and the eastern Indian Ocean (Kamenkovich et al. 2003, 2009) and more precisely by Eq. (31) in Burnett et al. (2003). Based on the analysis of momentum balance, previous studies have revealed that the ITF is generally in geostrophic balance, and its total transport is largely, but not uniquely, determined by the Pacific–Indian Ocean pressure head (Burnett et al. 2000a,b, 2003; Kamenkovich et al. 2003). Particularly, Kamenkovich et al. (2009) found that the ITF seasonality is highly correlated with the pressure head variations. Unfortunately, none of these studies investigated the influences of the SCSTF on the ITF pressure head through the Mindoro–Sibutu Passage because all their regional models excluded the SCS and the Sulu Sea. Our model results suggested that the Mindoro–Sibutu flow inputs buoyant SCS water into the western Sulawesi Sea and alters the pressure forces at the Pacific side boundary. This pressure head mechanism through the Mindoro–Sibutu Passage, which was originally proposed by Gordon et al. (2012) and recently examined by Qin et al. (2016) using SSH data, has been reproduced numerically in this study.

Although Gordon et al. (2012) emphasizes the interannual time scale, our results revealed that this mechanism is valid on the ITF seasonality too (Fig. 7b). Furthermore, the mechanism could also explain the enhanced seasonality and transport of the Makassar ITF during 2008–11 (illustrated in Fig. 2a of Gordon et al. 2012). Figure 13 displays up-to-date Makassar ITF measurements from 2004 to 2016. According to the Niño-3.4 index (Fig. 13b), 2008–12 was a prolonged La Niña period, during which the Mindoro–Sibutu flow was significantly reduced with less Luzon Strait intrusions. Thus, the Makassar ITF's seasonality is more determined by the Mindanao–Sulawesi flow with larger seasonality (Fig. 6f). On the other hand, the ITF seasonality and transport are reduced from 2004 to 2007 and from 2014 to 2016 (Fig. 13a), both of which periods are dominated by strong El Niño events. During El Niño years, enhanced Luzon Strait intrusion pushes more freshwater into the Mindoro–Sibutu Passage and consequently the Sulawesi Sea, leading to a relatively weaker ITF seasonality and transport. Even though the mooring data between September 2011 and July 2013 are missing (no mooring deployed), the correlation between the ITF and Niño-3.4 index is evident.

Acknowledgments. Jun Wei was supported by National Natural Science Foundation of China (Grant 41476008) and the Strategic Priority Research Program of the Chinese Academy of Sciences (Grants XDA11010303 and XDA11010302), and Paola Malanotte-Rizzoli was supported by the Singapore–MIT Alliance for Research and Technology under the CANSAM program. The funding for A. L. Gordon is derived from the Climate Program Office, Office of Climate Observation, National Oceanic and Atmospheric Administration, U.S. Department of Commerce. The statements, findings, conclusions, and recommendations are those of the author(s) and do not necessarily reflect the views of the National Oceanic and Atmospheric Administration or the Department of Commerce.

REFERENCES

Arruda, W. Z., and D. Nof, 2003: The Mindanao and Halmahera eddies—Twin eddies induced by nonlinearities. *J. Phys. Oceanogr.*, **33**, 2815–2830, doi:10.1175/1520-0485(2003)033<2815:TMAHEE>2.0.CO;2.

Berntsen, J., and L.-Y. Oey, 2010: Estimation of the internal pressure gradient in σ-coordinate ocean models: Comparison of second-, fourth-, and sixth-order schemes. *Ocean Dyn.*, **60**, 317–330, doi:10.1007/s10236-009-0245-y.

Burnett, W. H., V. M. Kamenkovich, D. A. Jaffe, A. L. Gordon, and G. L. Mellor, 2000a: Dynamical balance in the Indonesian seas circulation. *Geophys. Res. Lett.*, **27**, 2705–2708, doi:10.1029/2000GL011494.

——, ——, G. L. Mellor, and A. L. Gordon, 2000b: The influence of the pressure head on the Indonesian seas circulation. *Geophys. Res. Lett.*, **27**, 2273–2276, doi:10.1029/1999GL010918.

——, ——, A. L. Gordon, and G. L. Mellor, 2003: The Pacific/Indian Ocean pressure difference and its influence on the Indonesian seas circulation: Part I—The study with specified total transports. *J. Mar. Res.*, **61**, 577–611, doi:10.1357/002224003771815963.

Carton, J. A., G. Chepurin, and X. Cao, 2000: A Simple Ocean Data Assimilation analysis of the global upper ocean 1950–95. Part II: Results. *J. Phys. Oceanogr.*, **30**, 311–326, doi:10.1175/1520-0485(2000)030<0311:ASODAA>2.0.CO;2.

Ganachaud, A., and C. Wunsch, 2000: The oceanic meridional overturning circulation, mixing, bottom water formation, and heat transport. *Nature*, **408**, 453–457, doi:10.1038/35044048.

Godfrey, J. S., 1989: A Sverdrup model of the depth-integrated flow for the World Ocean allowing for island circulations. *Geophys. Astrophys. Fluid Dyn.*, **45**, 89–112, doi:10.1080/03091928908208894.

Gordon, A. L., 1986: Interocean exchange of thermocline water. *J. Geophys. Res.*, **91**, 5037–5046, doi:10.1029/JC091iC04p05037.

——, 2001: Interocean exchange. *Ocean Circulation and Climate*, G. Siedler, J. Church, and J. Gould, Eds., Academic Press, 303–314.

——, C. F. Giulivi, and A. G. Ilahude, 2003: Deep topographic barriers within the Indonesian seas. *Deep-Sea Res. II*, **50**, 2205–2228, doi:10.1016/S0967-0645(03)00053-5.

——, R. D. Susanto, A. Ffield, B. A. Huber, W. Pranowo, and S. Wirasantosa, 2008: Makassar Strait Throughflow, 2004 to 2006. *Geophys. Res. Lett.*, **35**, L24605, doi:10.1029/2008GL036372.

——, and Coauthors, 2010: The Indonesian Throughflow during 2004–2006 as observed by the INSTANT program. *Dyn. Atmos. Oceans*, **50**, 115–128, doi:10.1016/j.dynatmoce.2009.12.002.

——, B. A. Huber, E. J. Metzger, R. D. Susanto, H. E. Hurlburt, and T. R. Adi, 2012: South China Sea Throughflow impact on the Indonesian Throughflow. *Geophys. Res. Lett.*, **39**, L11602, doi:10.1029/2012GL052021.

——, P. Flament, C. Villanoy, and L. Centurioni, 2014: The nascent Kuroshio of Lamon Bay. *J. Geophys. Res. Oceans*, **119**, 4251–4263, doi:10.1002/2014JC009882.

Hirst, A. C., and J. S. Godfrey, 1993: The role of the Indonesian Throughflow in a global GCM. *J. Phys. Oceanogr.*, **23**, 1057–1086, doi:10.1175/1520-0485(1993)023<1057:TROITI>2.0.CO;2.

Hu, D., W. Cai, A. Ganachaud, W. S. Kessler, and J. Sprintall, 2015: Introduction to special section on western Pacific Ocean circulation and climate. *J. Geophys. Res. Oceans*, **120**, 3175–3176, doi:10.1002/2015JC010856.

Hu, S., D. Hu, C. Guan, F. Wang, L. Zhang, F. Wang, and Q. Wang, 2016: Interannual variability of the Mindanao Current/Undercurrent in direct observations and numerical simulations. *J. Phys. Oceanogr.*, **46**, 483–499, doi:10.1175/JPO-D-15-0092.1.

Hurlburt, H., E. Metzger, J. Sprintall, S. Riedlinger, R. Arnone, and T. Shinoda, 2011: Circulation in the Philippine Archipelago simulated by 1/12° and 1/25° global HYCOM and EAS NCOM. *Oceanography*, **24**, 28–47, doi:10.5670/oceanog.2011.02.

Kamenkovich, V. M., H. W. Burnett, A. L. Gordon, and G. L. Mellor, 2003: The Pacific/Indian Ocean pressure difference and its influence on the Indonesian seas circulation: Part II—The study with specified sea-surface heights. *J. Mar. Res.*, **61**, 613–634, doi:10.1357/002224003771815972.

——, K. T. A. O'Driscoll, and D. A. Nechaev, 2009: Dynamics of the Indonesian seas circulation. Part II—The role of pressure head. *J. Mar. Res.*, **67**, 159–184, doi:10.1357/002224009789051209.

Kim, Y. Y., T. Qu, T. Jensen, T. Miyama, H. Mitsudera, H.-W. Kang, and A. Ishida, 2004: Seasonal and interannual variations of the North Equatorial Current bifurcation in a high-resolution OGCM. *J. Geophys. Res.*, **109**, C03040, doi:10.1029/2003JC002013.

Lien, R.-C., and Coauthors, 2015: The Kuroshio and Luzon Undercurrent east of Luzon Island. *Oceanography*, **28**, 54–63, doi:10.5670/oceanog.2015.81.

Liu, Q. Y., R. Huang, D. Wang, Q. Xie, and Q. Huang, 2006: Interplay between the Indonesian Throughflow and the South China Sea Throughflow. *Chin. Sci. Bull.*, **51**, 50–58, doi:10.1007/s11434-006-9050-x.

——, M. Feng, and D. Wang, 2011: ENSO-induced interannual variability in the southeastern South China Sea. *J. Oceanogr.*, **67**, 127–133, doi:10.1007/s10872-011-0002-y.

——, R. X. Huang, and D. X. Wang, 2012: Implication of the South China Sea Throughflow for the interannual variability of the regional upper-ocean heat content. *Adv. Atmos. Sci.*, **29**, 54–62, doi:10.1007/s00376-011-0068-x.

Masumoto, Y., and T. Yamagata, 1993: Simulated seasonal circulation in the Indonesian seas. *J. Geophys. Res.*, **98**, 12 501–12 509, doi:10.1029/93JC01025.

——, and Coauthors, 2004: A fifty-year eddy-resolving simulation of the world ocean—Preliminary outcomes of OFES (OGCM for the Earth Simulator). *J. Earth Simul.*, **1**, 35–56.

Mellor, G. L., and T. Yamada, 1982: Development of a turbulence closure model for geophysical fluid problem. *Rev. Geophys. Space Phys.*, **20**, 851–875, doi:10.1029/RG020i004p00851.

Metzger, E. J., and H. E. Hurlburt, 1996: Coupled dynamics of the South China Sea, the Sulu Sea, and the Pacific Ocean. *J. Geophys. Res.*, **101**, 12 331–12 352, doi:10.1029/95JC03861.

Oey, L. Y., and P. Chen, 1992a: A model simulation of circulation in the northeast Atlantic shelves and seas. *J. Geophys. Res.*, **97**, 20 087–20 115, doi:10.1029/92JC01990.

——, and ——, 1992b: A nested-grid ocean model: With application to the simulation of meanders and eddies in the Norwegian Coastal Current. *J. Geophys. Res.*, **97**, 20 063–20 086, doi:10.1029/92JC01991.

——, T. Ezer, D. P. Wang, S. J. Fan, and X. Q. Yin, 2006: Loop Current warming by Hurricane Wilma. *Geophys. Res. Lett.*, **33**, L08613, doi:10.1029/2006GL025873.

——, ——, ——, X. Q. Yin, and S. J. Fan, 2007: Hurricane-induced motions and interaction with ocean currents. *Cont. Shelf Res.*, **27**, 1249–1263, doi:10.1016/j.csr.2007.01.008.

——, Y. L. Chang, Y. C. Lin, M. C. Chang, F. H. Xu, and H. F. Lu, 2013: ATOP—The Advanced Taiwan Ocean Prediction System based on the mpiPOM Part 1: Model descriptions, analyses and results. *Terr. Atmos. Oceanic Sci. J.*, **24**, 137–158, doi:10.3319/TAO.2012.09.12.01(Oc).

——, ——, ——, ——, S. Varlamov, and Y. Miyazawa, 2014: Cross flows in the Taiwan Strait in winter. *J. Phys. Oceanogr.*, **44**, 801–817, doi:10.1175/JPO-D-13-0128.1.

Pujiana, K., A. L. Gordon, and J. Sprintall, 2013: Intraseasonal Kelvin wave in Makassar Strait. *J. Geophys. Res. Oceans*, **118**, 2023–2034, doi:10.1002/jgrc.20069.

Qiu, B., and R. Lukas, 1996: Seasonal and interannual variability of the North Equatorial Current, the Mindanao Current, and the Kuroshio along the Pacific western boundary. *J. Geophys. Res.*, **101**, 12 315–12 330, doi:10.1029/95JC03204.

——, and S. Chen, 2010: Interannual-to-decadal variability in the bifurcation of the North Equatorial Current off the Philippines. *J. Phys. Oceanogr.*, **40**, 2525–2538, doi:10.1175/2010JPO4462.1.

——, D. L. Rudnick, I. Cerovecki, B. D. Cornuelle, S. Chen, M. C. Schönau, J. L. McClean, and G. Gopalakrishnan, 2015: The Pacific North Equatorial Current: New insights from the origins of the Kuroshio and Mindanao Currents (OKMC) project. *Oceanography*, **28**, 24–33, doi:10.5670/oceanog.2015.78.

Qin, H., R. X. Huang, W. Wang, and H. Xue, 2016: Regulation of South China Sea throughflow by pressure difference. *J. Geophys. Res. Oceans*, **121**, 4077–4096, doi:10.1002/2015JC011177.

Qu, T., and Y. T. Song, 2009: Mindoro Strait and Sibutu Passage transports estimated from satellite data. *Geophys. Res. Lett.*, **36**, L09601, doi:10.1029/2009GL037314.

——, H. Mistudera, and T. Yamagata, 1998: On the western boundary currents in the Philippine Sea. *J. Geophys. Res.*, **103**, 7537–7548, doi:10.1029/98JC00263.

——, Y. Y. Kim, M. Yaremchuk, T. Tozuka, A. Ishida, and T. Yamagata, 2004: Can Luzon Strait transport play a role in conveying the impact of ENSO to the South China Sea? *J. Climate*, **17**, 3644–3657, doi:10.1175/1520-0442(2004)017<3644:CLSTPA>2.0.CO;2.

——, Y. Du, G. Meyers, A. Ishida, and D. Wang, 2005: Connecting the tropical Pacific with Indian Ocean through South China Sea. *Geophys. Res. Lett.*, **32**, L24609, doi:10.1029/2005GL024698.

——, Y. T. Song, and T. Ymagata, 2009: An introduction to the South China Sea Throughflow: Its dynamics, variability, and application for climate. *Dyn. Atmos. Oceans*, **47**, 3–14, doi:10.1016/j.dynatmoce.2008.05.001.

Rudnick, D. L., S. Jan, and C. M. Lee, 2015: A new look at circulation in the western North Pacific. *Oceanography*, **28**, 16–23, doi:10.5670/oceanog.2015.77.

Schönau, M. C., and D. L. Rudnick, 2015: Glider observations of the North Equatorial Current in the western tropical Pacific. *J. Geophys. Res. Oceans*, **120**, 3586–3605, doi:10.1002/2014JC010595.

Semtner, A. J., and R. M. Chervin, 1988: A simulation of the global circulation with resolved eddies. *J. Geophys. Res.*, **93**, 15 502–15 522, doi:10.1029/JC093iC12p15502.

Sheremet, V. A., 2001: Hysteresis of a western boundary current leaping across a gap. *J. Phys. Oceanogr.*, **31**, 1247–1259, doi:10.1175/1520-0485(2001)031<1247:HOAWBC>2.0.CO;2.

Smagorinsky, J., 1963: General circulation experiments with the primitive equations. I. The basic experiment. *Mon. Wea. Rev.*, **91**, 99–164, doi:10.1175/1520-0493(1963)091<0099:GCEWTP>2.3.CO;2.

Sprintall, J., and A. Revelard, 2014: The Indonesian Throughflow response to Indo-Pacific climate variability. *J. Geophys. Res. Oceans*, **119**, 1161–1175, doi:10.1002/2013JC009533.

——, A. L. Gordon, R. Murtugudde, and R. D. Susanto, 2000: A semiannual Indian Ocean forced Kelvin wave observed in the Indonesian seas in May 1997. *J. Geophys. Res.*, **105**, 17 217–17 230, doi:10.1029/2000JC900065.

——, and Coauthors, 2004: INSTANT: A new international array to measure the Indonesian Throughflow. *Eos, Trans. Amer. Geophys. Union*, **85**, 369–376, doi:10.1029/2004EO390002.

——, G. Siedler, and H. Mercier, 2013: Inter-ocean and interbasin exchanges. *Ocean Circulation and Climate: A 21st Century Perspective*, G. Siedler, S. M. Griffies, J. Gould, and J. A. Church, Eds., 493–552.

——, A. L. Gordon, A. Koch-Larrouy, T. Lee, J. T. Potemra, K. Pujiana, and S. E. Wijffels, 2014: The Indonesian seas and their impact on the coupled ocean–climate system. *Nat. Geosci.*, **7**, 487–492, doi:10.1038/ngeo2188.

Tian, J., Q. Yang, X. Liang, D. Hu, F. Wang, and T. Qu, 2006: The observation of Luzon Strait transport. *Geophys. Res. Lett.*, **33**, L19607, doi:10.1029/2006GL026272.

Tozuka, T., T. Qu, and T. Yamagata, 2007: Dramatic impact of the South China Sea on the Indonesian Throughflow. *Geophys. Res. Lett.*, **34**, L12612, doi:10.1029/2007GL030420.

——, ——, Y. Masumoto, and T. Yamagata, 2009: Impacts of the South China Sea Throughflow on seasonal and interannual variations of the Indonesian Throughflow. *Dyn. Atmos. Oceans*, **47**, 73–85, doi:10.1016/j.dynatmoce.2008.09.001.

Tranchant, B., G. Reffray, E. Greiner, D. Nugroho, A. Koch-Larrouy, and P. Gaspar, 2016: Evaluation of an operational ocean model configuration at 1/12° spatial resolution for the Indonesian seas (NEMO2.3/INDO12)—Part 1: Ocean physics. *Geosci. Model Dev.*, **9**, 1037–1064, doi:10.5194/gmdd-8-6611-2015.

Van Sebille, E, J. Sprintall, F. U. Schwarzkopf, A. Sen Gupta, A. Santoso, M. H. England, A. Biastoch, and C. W. Böning, 2014: Pacific-to-Indian Ocean connectivity: Tasman leakage, Indonesian Throughflow, and the role of ENSO. *J. Geophys. Res. Oceans*, **119**, 1365–1382, doi:10.1002/2013JC009525.

Wang, Z., and D. Yuan, 2012: Nonlinear dynamics of two western boundary currents colliding at a gap. *J. Phys. Oceanogr.*, **42**, 2030–2040, doi:10.1175/JPO-D-12-05.1.

——, and ——, 2014: Multiple equilibria and hysteresis of two unequal-transport western boundary currents colliding at a gap. *J. Phys. Oceanogr.*, **44**, 1873–1885, doi:10.1175/JPO-D-13-0234.1.

Wyrtki, K., 1961: *Physical Oceanography of the Southeast Asian Waters*. NAGA Rep., Vol. 2, Scripps Institute of Oceanography, 195 pp.

——, 1973: An equatorial jet in the Indian Ocean. *Science*, **181**, 262–264, doi:10.1126/science.181.4096.262.

Xu, D., and P. Malanotte-Rizzoli, 2013: The seasonal variation of the upper layers of the South China Sea (SCS) circulation and the Indonesian Through flow (ITF): An ocean model study. *Dyn. Atmos. Oceans*, **63**, 103–130, doi:10.1016/j.dynatmoce.2013.05.002.

Yaremchuk, M., and T. Qu, 2004: Seasonal variability of the large-scale currents near the coast of the Philippines. *J. Phys. Oceanogr.*, **34**, 844–855, doi:10.1175/1520-0485(2004)034<0844:SVOTLC>2.0.CO;2.

Yu, L., and R. A. Weller, 2007: Objectively analyzed air–sea heat fluxes for the global ice-free oceans (1981–2005). *Bull. Amer. Meteor. Soc.*, **88**, 527–539, doi:10.1175/BAMS-88-4-527.

Zeng, L., W. T. Liu, H. Xue, P. Xiu, and D. Wang, 2014: Freshening in the South China Sea during 2012 revealed by *Aquarius* and in situ data. *J. Geophys. Res. Oceans*, **119**, 8296–8314, doi:10.1002/2014JC010108.

Zhang, L. L., D. X. Hu, S. Hu, F. Wang, F. Wang, and D. Yuan, 2014: Mindanao Current/Undercurrent measured by a subsurface mooring. *J. Geophys. Res. Oceans*, **119**, 3617–3628, doi:10.1002/2013JC009693.